World Journal of Radiology

Online Submissions: http://www.wjgnet.com/1949-8470office
wjr@wjgnet.com
doi:10.4329/wjr.v2.i8.309

World J Radiol 2010 August 28; 2(8): 309-322
ISSN 1949-8470 (online)

REVIEW

Magnetic resonance imaging: Review of imaging techniques and overview of liver imaging

Santhi Maniam, Janio Szklaruk

Santhi Maniam, Janio Szklaruk, Department of Diagnostic Radiology, University of Texas M. D. Anderson Cancer Center, Houston, TX 77030, United States
Author contributions: Both authors contribute the research, text, organization, editing, and revision of the manuscript.
Correspondence to: Janio Szklaruk, MD, PhD, Department of Diagnostic Radiology, University of Texas M. D. Anderson Cancer Center, 1515 Holcombe, Box 368, Houston, TX 77030, United States. jszklaru@mdanderson.org
Telephone: +1-713-7451453 Fax: +1-713-7451302
Received: May 20, 2010 Revised: June 24, 2010
Accepted: July 15, 2010
Published online: August 28, 2010

Abstract

Magnetic resonance imaging (MRI) of the liver is slowly transitioning from a problem solving imaging modality to a first line imaging modality for many diseases of the liver. The well established advantages of MRI over other cross sectional imaging modalities may be the basis for this transition. Technological advancements in MRI that focus on producing high quality images and fast imaging, increasing diagnostic accuracy and developing newer function-specific contrast agents are essential in ensuring that MRI succeeds as a first line imaging modality. Newer imaging techniques, such as parallel imaging, are widely utilized to shorten scanning time. Diffusion weighted echo planar imaging, an adaptation from neuroimaging, is fast becoming a routine part of the MRI liver protocol to improve lesion detection and characterization of focal liver lesions. Contrast enhanced dynamic T1 weighted imaging is crucial in complete evaluation of diseases and the merit of this dynamic imaging relies heavily on the appropriate timing of the contrast injection. Newer techniques that include fluoro-triggered contrast enhanced MRI, an adaptation from 3D MRA imaging, are utilized to achieve good bolus timing that will allow for optimum scanning. For accurate interpretation of liver diseases, good understanding of the newer imaging techniques and familiarity with typical imaging features of liver diseases are essential. In this review, MR sequences for a time efficient liver MRI protocol utilizing newer imaging techniques are discussed and an overview of imaging features of selected common focal and diffuse liver diseases are presented.

Key words: Magnetic resonance imaging; Liver; Oncology; Contrast agents

Peer reviewers: Rajasvaran Logeswaran, PhD, Associate Professor, Faculty of Engineering, Multimedia University, 63100 Cyberjaya, Malaysia; Kenneth Coenegrachts, MD, PhD, Department of Radiology, AZ St.-Jan AV, Ruddershove 10, B-8000 Bruges, Belgium

Maniam S, Szklaruk J. Magnetic resonance imaging: Review of imaging techniques and overview of liver imaging. *World J Radiol* 2010; 2(8): 309-322 Available from: URL: http://www.wjgnet.com/1949-8470/full/v2/i8/309.htm DOI: http://dx.doi.org/10.4329/wjr.v2.i8.309

INTRODUCTION

Magnetic resonance imaging (MRI) of the abdomen has been routinely performed to further characterize indeterminate lesions seen on other cross sectional imaging, such as ultrasound (US) and computed tomography (CT). However, MRI is increasingly used as the principal diagnostic modality, especially for staging and restaging of oncologic patients. With advancement of technology and development of newer imaging techniques, MRI of the abdomen allows for near optimal evaluation of, not only the liver, but also most of the other organs in the abdomen, retroperitoneal structures and even the peritoneum[1].

One of the obstacles to optimal MRI of the abdomen is periodic motion associated with respiratory movement and the historic long examinations. To overcome this limitation, novel imaging techniques, such as parallel imag-

ing (PI), have allowed for shorter breath hold sequences without significant loss in the signal to noise ratio (SNR)[2-4]. Although to a lesser degree than on CT or US, a limitation of liver MRI has been the overlap of imaging features of various disease processes that render them as indeterminate findings. Incorporation of newer imaging techniques (such as PI) and new contrast agents (such as hepatocyte agents) have improved the diagnostic accuracy of MRI, for example, the utilization of diffusion weighted echo planar imaging (EPI), which had been standard practice in neuroimaging. The enhancement pattern at different phases after contrast administration can be crucial for the detection and characterization of liver pathology. The addition of the hepatocyte phase after contrast administration has permitted increased discrimination between liver and non-hepatocyte containing lesions. In this review, we discuss the design of a time-efficient MR protocol and the justification for various sequences and techniques for optimum liver imaging. We present the specific imaging features of selected common focal and diffuse liver diseases utilizing this model MR protocol technique[1].

MRI TECHNIQUES

Axial T1 weighted spoiled gradient echo in-phase and opposed-phase

Historically, T1 weighted imaging (T1WI) of the liver have been obtained with a spin-echo technique. Although this technique provided exquisite SNR and minimum artifacts, the scan time could be considered as prohibitive. Currently, routine T1WI evaluation is obtained with spoiled gradient echo (SPGR) techniques (GE Medical Systems, Milwaukee, WI; fast low-angle shot sequences, Siemens Medical Systems, Erlangen, Germany). The imaging parameters for this sequence with a 1.5T magnet were TE = 4.2 ms and 2.1 ms with TR = 100 ms. For the 3T magnets, a TE of 2.1 ms and 4.2 ms correspond to in-phase (IP) and out-of-phase (OP) imaging, respectively. The slice thickness was 5 mm/0 mm gap. Utilizing a double echo technique, IP and OP images were obtained in one TR. At 1.5T, an echo time of 4.2 ms resulted in a predominantly IP image (water and fat signal are added), with a 2.1 ms echo time, water and fat signal cancel each other resulting in out of phase image. The addition of PI (see discussion on PI below) to the image acquisition parameters resulted in a scan time of 14-18 s, which was short enough for a breath hold in most patients, to cover the entire abdomen[5].

The normal signal of the liver on T1WI is slightly hyperintense to muscle and kidneys. The signal was variable depending on the fat and iron content of the liver. In a fatty liver, the signal of the liver in the IP T1WI is slightly hyperintense. In a liver with high iron content, the signal on the IP T1WI is slightly hypointense.

Axial T2 weighted imaging

The use of fast spin echo (FSE) techniques with a multiple echo train has significantly shortened scan times[6]. However, scan time reduction comes at the expense of the contrast to noise ratio (CNR) and SNR[7]. To minimize mis-registration, a respiratory triggered FSE (RT-FSE) T2 weighted imaging (T2WI) sequence is preferred[8]. A respiratory triggered technique with an echo train length (ETL) of 16-20 provides excellent T2WI. Longer ETL (> 20) may result in loss of CNR between the lesion and liver. A TE of 80-90 ms results in high quality images with an optimal combination of high SNR and CNR[7]. Modification of the echo time to longer TE (150-250 ms) has been used to discriminate between cysts (long T2 relaxation masses) and solid lesions (relatively shorter T2 relaxation masses[9,10].

The T2WI can also be obtained with breath hold techniques. The fast recovery FSE techniques (FRFSE, GE Medical Systems) can provide good breath hold T2WI contrast with improved scan times[8]. This pulse sequence includes recovery of the compulsory longitudinal magnetization. The T2WI (RT-FSE or FRFSE) are obtained with fat-saturation. The fat suppression is achieved with frequency selective techniques.

The imaging parameters for T2 weighted RT-FSE comprise TR = 4000-6000 ms and TE = 85 ms. The number of excitations is 3-4. The slice thickness/gap is 6 mm/0 mm. The imaging parameters for FRFSE were comprised of TE = 85 ms and TR = 2000 ms.

The normal signal of the liver on T2WI is hypointense to the spleen, kidneys, and pancreas. In contrast, most of the liver pathology is hyperintense to the liver parenchyma. This has been very useful since the early days of liver MR.

Diffusion weighted imaging

Neuroimaging has used diffusion weighted imaging (DWI) in the detection and characterization of brain lesions. This has been successfully applied to the evaluation of the liver. The principle is to apply two identical diffusion-sensitizing gradient pulses separated by a 180° refocusing pulse to a T2 weighted sequence. Stationary protons are unaffected by the gradient pulses because the phase shift acquired on the first pulse is reversed by the second pulse with an end result of no phase shift, which means no signal is lost. On the contrary, moving protons acquire a phase shift from the first gradient, which is not completely reversed by the second gradient pulse, which results in signal loss. Diffusion of protons thus is visually perceived as signal attenuation on the diffusion weighted images. EPI is used to obtain the T2WI for DWI. The EPI can be obtained with a breath hold, free-breathing, or respiratory triggered techniques. The respiratory triggered EPI is preferred over breath-hold EPI for SNR reasons. The diffusion gradients are best obtained in three orthogonal planes but, in the liver, adequate images can be obtained with only one axis (z-axis) gradient. DWI of at least two b-values are performed (b = 0 or 500 s/mm^2). The higher b-value image will result in the reduction of signal from moving protons in the bile ducts, cysts, vessels, and fluid in the bowel. This will result in an increased contrast between the lesion and liver. Visual assessment is of value to distin-

guish cystic from solid lesions, however, to distinguish benign and malignant solid lesions is often difficult. Another confounding factor in visual tumor assessment is that the signal intensity of a lesion is dependent on both water proton diffusion and the T2-relaxation time. Thus a lesion may have a high signal on DWI, suggesting diffusion restriction, when in fact it is due to the tissue's intrinsic long T2 relaxation time; a phenomenon called T2 shine-through effect. Since DWI is originally a T2 weighted sequence, the DWI imaging should be interpreted, along with other standard sequences and especially the standard T2 weighted sequences, to avoid this potential error[11-13]. DWI at low b-value (50 s/mm^2) (yes) results in black blood images of the liver that facilitates identification of small focal liver lesions (< 10 mm) from the dark intrahepatic vessels[14].

The imaging parameters for the DWI EPI using a breath hold technique and PI with multi-channel phased array coil are: TR/TE (1200-1800 s/50-60 s); FOV (38-44 cm); matrix (200 × 160); number of excitations (NEX-6); slice thickness (7 mm/0 mm); two acquisitions obtained for b-values of 0 and 500 s/mm^2 with a scan time of 21 s.

The normal signal of the liver on DWI is the same as on other T2WI. The liver is hypointense to the kidneys and pancreas.

Parallel imaging

PI is an accelerated imaging technique that combines available MRI methods and newly developed multi-channel phased array coils to significantly reduce scanning time. In PI techniques, under sampled k-space, data in the phase encoding direction are acquired to shorten scanning time. These incomplete data are supplemented by the spatial information encoded by the multi-channeled phase array surface coils to complete the MRI. Theoretically, the maximum acceleration factor is limited by the number of coil elements. Practically, the acceleration factor is currently limited by a factor of 2 to 4, which results in high quality images[14].

Different parallel reconstruction algorithms, such as ASSET (GEMS), SENSE (Phillips), and SMASH (Siemens), are used to generate unaliased final images[5,15]. The PI technique improves breath hold imaging by eliminating periodic respiratory motion artifacts due to fast imaging with subsequent increased spatial resolution. Acceleration factors of 2 to 3 are commonly used. The important limiting factor of PI is loss of SNR with improving resolution[16].

Dynamic axial T1 weighted FSPGR LAVA contrast enhanced imaging

Dynamic contrast enhanced (DCE)-MRI of the liver is a vital part of the liver imaging protocol due to its greater diagnostic accuracy. Given the distinctive liver physiology and its dual blood supply, dynamic enhancement patterns for a particular disease on the different phases of liver enhancement can narrow the differential diagnosis.

Images are acquired in three phases following contrast administration: a predominant arterial (or late arterial) phase, portal phase, and a delayed (equilibrium) phase. The first phase is the most time sensitive phase. The timing for the portal venous and delayed phases is less critical. To optimize the capture of this first phase of enhancement, novel techniques have been developed.

For example, a less preferred method uses a standard delay of 20 s following the administration of contrast. This method does not compensate for cardiac output or other physiologic delays. A second method is to do a timing bolus. This is performed with a small amount (1-2 mL) that is injected while a single slice of the abdomen is monitored during the entire injection to determine the appropriate delay time for the contrast to arrive to the liver. The main limitations are longer scans and the introduction of contrast prior to the complete exam. A third method is to obtain two consecutive arterial phases following contrast administration after a preset short delay[17]. This requires a decrease in spatial resolution to shorten the scan time[18]. Finally, fluoro-triggered images provide an alternative method to visualize the contrast injection and set a short delay after the visualization of contrast in the aorta or pulmonary arteries.

To calculate the optimum delay in these methods, it is important to have knowledge of the k-space filling method of the MR software. A platform with the first echo at the center of k-space will be at a different stage of enhancement compared to a method where the center of k-space is obtained in the middle of the acquisition[18,19]. The image contrast relies mainly on data acquired near the center of the k-space, while the image edge sharpness depends on data from the periphery of the k-space. The development of a new method of imaging, such as the key-hole method, allows for merging of high frequency k-space data from a reference image acquired with a reduced matrix. This data merging method combines the spatial resolution of full matrix images and the temporal resolution of a set of rapidly acquired, reduced matrix images. The key-hole method thus yields images with high temporal resolution without significantly compromised spatial resolution[20-22].

DCE-MRI of the liver is performed using a 3D axial T1 weighted fast SPGR LAVA (GEMS) sequence with the following parameters: TE > 1.5 ms; FOV (34-44 cm), matrix [320 × (160-192)], slice thickness (4-5 mm), Zerofill interpolation processing 2 breath-hold technique with PI used during triphasic acquisition of the entire abdomen after contrast infusion at late arterial, portal venous, and delayed phase of contrast administration.

Hepatocyte specific gadolinium based contrast agent (Gd-EOB-DTPA)

Gd-EOB-DTPA (known as Eovist, Primovist and EOB-Primovist, Bayer Pharmaceuticals) is a paramagnetic, highly water soluble, hydrophilic compound that has a lipophilic moiety, called an ethoxybenzyl group, covalently linked to the Gd-DTPA to form Gd-EOB-DTPA. Gd-EOB-DTPA is selectively taken up by hepatocytes *via* an anionic transporter protein, which makes it the first tissue specific gadolinium based contrast agent (GBCA). It is eliminated unchanged *via* two routes in equal quantities: one route

is *via* biliary excretion of contrast selectively taken up by hepatocytes and the other route is *via* urinary excretion of contrast after glomerular filtration in the kidney[23]. The recommended dose of Gd-EOB-DTPA is 0.025 mmol/kg of body weight, which is about one quarter of the standard dose of nonspecific GBCA. The relaxivity of Gd-EOB-DTPA is comparable to most nonspecific GBCA due to non covalent weak transient binding with serum albumin[3,22,23].

Gd-EOB-DTPA combines both features of extracellular contrast agent and hepatocyte specific contrast, which allows for DCE imaging due to its extracellular function and delayed static hepatobiliary imaging due to its hepatocyte specific function[20]. Therefore, in addition to tumor characterization based on perfusion in the dynamic phase, Gd-EOB-DTPA offers concurrent assessment during the hepatocyte phase for the presence of intralesional functioning hepatocytes[24]. The selective uptake by hepatocytes increases lesion to liver contrast particularly in the hepatocyte phase, which is not attainable with nonspecific GBCA. The peak liver enhancement using Gd-EOB-DTPA is best observed after 20 min[23]. A time delay of 20 min for the hepatocyte phase is a widely accepted duration and has been part of liver imaging protocols using Gd-EOB-DTPA. To shorten the overall examination time, a new suggestion of a shorter delay of 10 min for the hepatocyte phase with sufficient liver enhancement has been made in patients with normal liver function[20]. In patients with chronic liver disease, where suppressed and delayed liver enhancement in the hepatocyte phase is routinely observed, a 20 min delay for hepatocyte imaging is compulsory[20,23]. Another recommendation to reduce the total examination time is to acquire T2 weighted sequences (FSE, FRFSE, and DWI) after contrast administration[23].

COMMON FOCAL LIVER LESIONS

Simple liver cysts

Simple liver cysts are common benign livers lesions that are developmental in origin. They are usually incidental findings that do not require further workup[10]. At MR imaging, liver cysts are hypointense on T1WI and hyperintense on T2WI. They do not show enhancement at dynamic imaging or uptake of contrast in the hepatocyte phase. Most liver cysts, including sub centimeter cysts, usually can be diagnosed based on typical MRI features (Figure 1). However, when contraindicated, further characterization with non-contrast MRI is still possible. On T2WI, cysts tend to remain hyperintense or become more hyperintense than surrounding liver parenchyma at longer TE > 250 ms[10]. At DWI, cysts usually have high signal at b = 0 with signal attenuation at higher b-values. Unfortunately, due to the T2 shine through effect, cysts can remain hyperintense at higher b-values[25]. In this setting, an apparent diffusion coefficient (ADC) map will be very useful. For a simple cyst, an ADC of $2.61 \times 10^{-3}/mm^2$ per second will suggest a cyst *vs* a mean ADC of $1.31 \times 10^{-3}/mm^2$ per second for hepatomas[12,26]. Even though the use of ADC values has been proven to be useful, there still is significant overlap between different types of focal liver lesions.

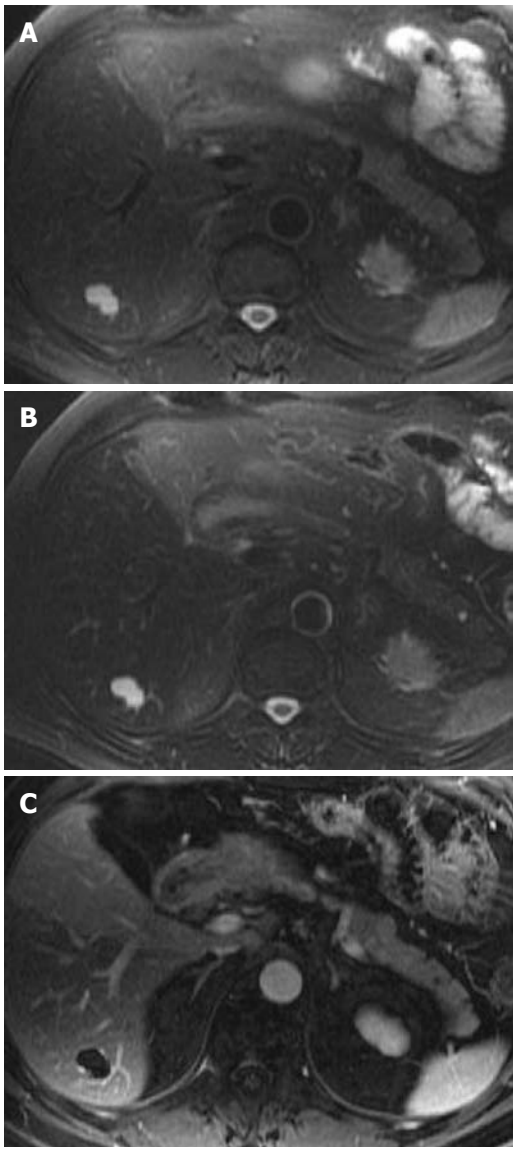

Figure 1 A 51-year-old male with colorectal cancer and liver cysts. A, B: The short (A, TE = 85 ms) and long (B, TE = 160 ms) respiratory triggered fast spin echo T2 weighted imaging demonstrates a stable contrast to noise ratio of lesion to liver; C: The post-gadolinium image shows no enhancement.

Hemangiomas

Hemangiomas are the most common solid benign liver lesions and are typically asymptomatic. At MR imaging, hemangiomas are classically hypointense on TIWI and hyperintense on T2WI. On T2WI with a longer echo time (TE = 140 ms), hemangiomas, like cysts, will remain hyperintense relative to the liver[27]. The CNR will not suffer as much with cysts and hemangiomas compared to other masses (Figure 2). On DWI, similar to cysts, hemangiomas will have high signal at b = 0 with a lesser degree of signal attenuation at higher b-values in the absence of the T2 shine through effect[27]. For hemangiomas, the mean ADC of $1.84 \times 10^{-3}/mm^2$ per second is between that of cysts and the ADC for hepatomas[12,26]. There is some

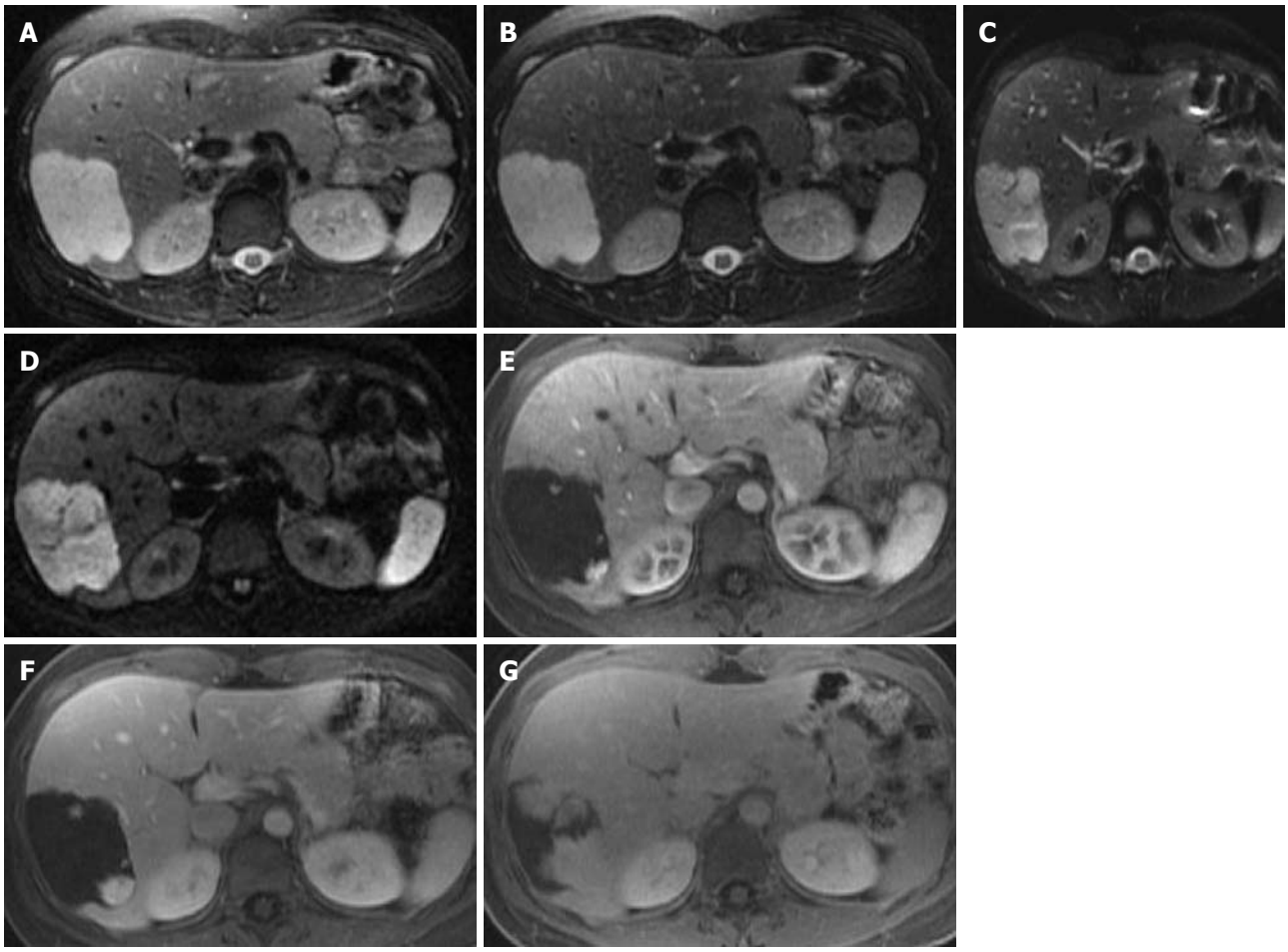

Figure 2 A 21-year-old female with right upper quadrant pain with a hemangioma. A, B: The short (A, TE = 85 ms) and long (B, TE = 160 ms) respiratory triggered fast spin echo T2 weighted imaging demonstrates a stable contrast to noise ratio of lesion to liver; C, D: The diffusion weighted imaging (C, b = 0, and D, b = 500) demonstrates high signal intensity of the hemangioma; E-G: The multiphasic post-Gd images demonstrate peripheral interrupted nodular enhancement with delayed fill-in, in the late arterial (E), portal venous (F), and excretory phase (G) of post-Gd images.

overlap between the ADC value of malignant lesions and hemangiomas[12,26].

Post-Gd imaging features of hemangiomas on DCE-MRI depend on their size. Three distinct dynamic enhancement patterns have been described. Pattern 1 is seen in small capillary hemangiomas < 1.5 cm and is typified by homogenous enhancement in early arterial enhancement with persistent enhancement on subsequent phases. Pattern 2 is seen in hemangiomas > 1.5 cm and is typified by classic peripheral nodular discontinuous enhancement in the arterial and portal phases with persistent enhancement peripherally with possible complete fill in on the delayed images (Figure 2). The second pattern is the most common and classic enhancement pattern of hemangiomas. Pattern 3 is seen in giant hemangiomas > 6 cm and is typified by peripheral nodular interrupted enhancement with gradual partial filling in on the arterial and portal phases but with a persistent hypointense center on delayed images. At the hepatocyte phase, no contrast is taken up by hemangiomas[27]. This can be challenging in the setting of hemangiomas and liver metastases, where both lesions will appear hypointense on the hepatocyte phase of contrast administration.

Focal nodular hyperplasia

Focal nodular hyperplasia (FNH) is the second most common benign liver lesion after hemangioma. They are thought to be a hyperplastic reaction to a congenital or acquired vascular malformation. On histopathology, they contain normal hepatocytes with malformed biliary tracts. They tend to be hypervascular lesions that often are incidental findings and are asymptomatic. FNH are grouped into two subtypes based on histology-classic (80%) and nonclassic (20%). At MR imaging, the classic imaging features on standard sequences are isointense on T1WI and T2WI with well formed central scars that are hyperintense on T2WI and are hypointense T1WI[4,28]. At DWI, they have variable signal intensity[29]. At DCE-MRI, they show intense enhancement in the arterial phase that returns to isointense to surrounding liver parenchyma in subsequent phases. The central scar has characteristic enhancement on the delayed images (Figure 3). The nonclassic type tends to lack the central scar, therefore, these FNH are isointense on T1WI and T2WI and show intense arterial enhancement on DCE-MRI that become isointense to background liver on subsequent phases[5,28]. One of the most common indications of liver MRI is to characterize

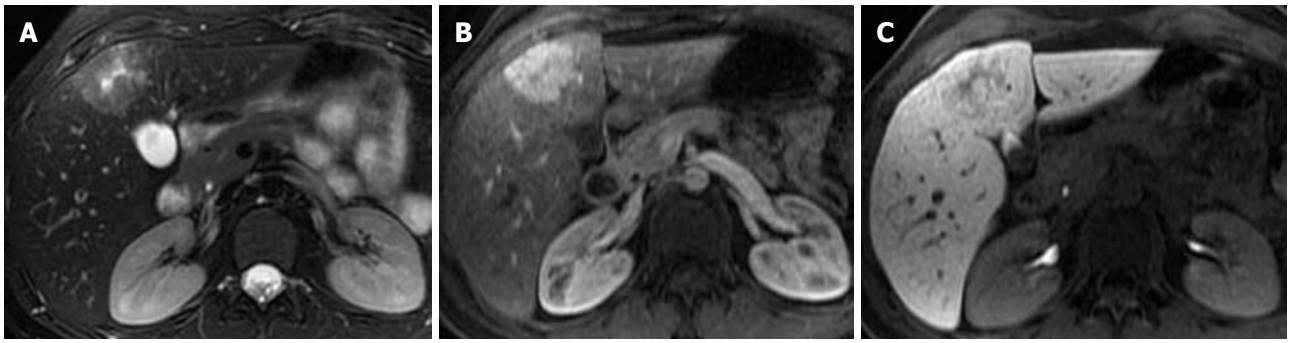

Figure 3 A 22-year-old female with an focal nodular hyperplasia in the liver. A: Respiratory triggered fast spin echo T2 weighted imaging at TE = 85 ms. This demonstrates a high signal in the center of the lesion; B: The late arterial phase of contrast administration shows hyperintense enhancement; C: The hepatocyte phase of contrast administration shows hepatocyte contrast uptake.

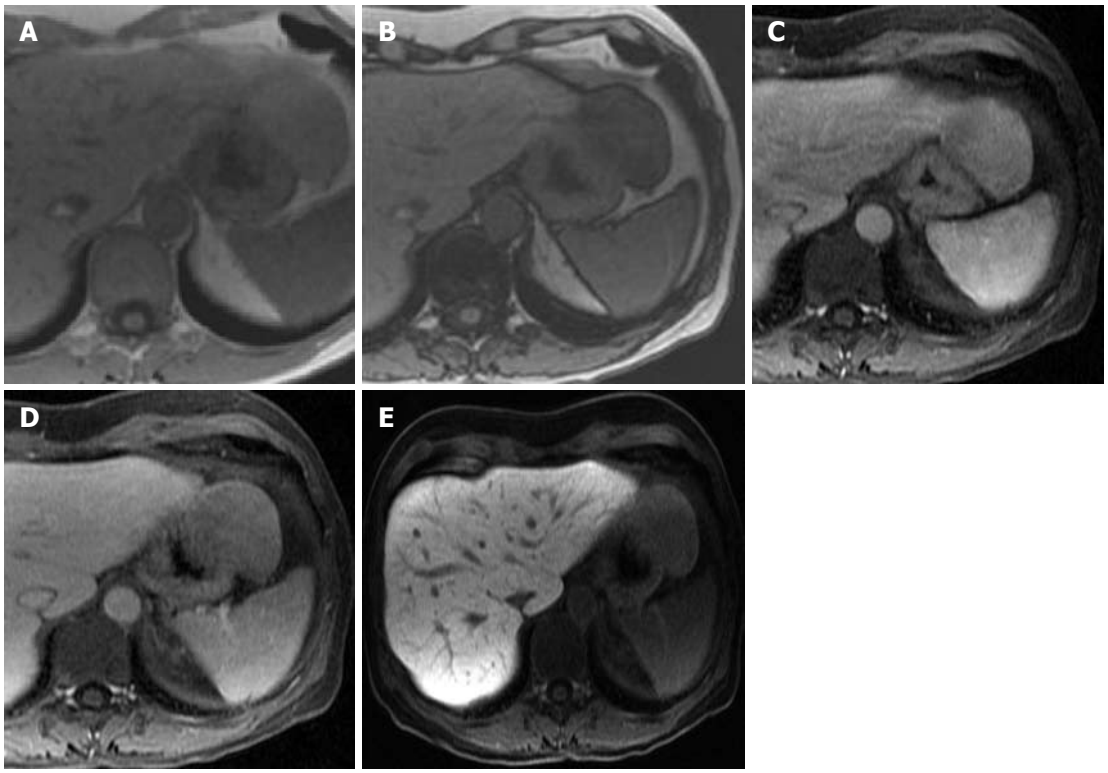

Figure 4 A 58-year-old female with a hepatic adenoma. A, B: In phase (A) and out-of-phase (B) T1 weighted imaging shows a signal drop in the adenoma on the out-of-phase image; C, D: Late arterial and delayed phase imaging demonstrates early enhancement (C) and delayed washout (D); E: The hepatocyte phase of contrast administration does not show uptake.

hypervascular lesions on CT or MRI that may represent an FNH. Hepatocyte agents are useful in this application of liver imaging. Given its hepatocellular origin, most FNH will appear isointense to hyperintense relative to surrounding liver at the hepatocyte phase (Figure 3). This is due to retention of contrast in dysfunctional bile ducts with poor drainage within the FNH[19].

Adenoma

Adenomas are rare benign liver neoplasms that occur commonly in women who are on oral contraceptives and with increased incidence in glycogen storage disease and with anabolic steroid use. Adenomas are usually symptomatic, however, they can be complicated by intralesional hemorrhage, rupture and rarely malignant transformation. Histopathologically, adenoma consists of hepatocytes arranged in plates that are separated by dilated sinusoids. A fibrous capsule or pseudocapsule consisting of compressed liver parenchyma is usually present. Portal triad and bile ducts are absent with minimal to complete absence of Kupffer cells. They contain variable amounts of glycogen and lipids[28]. At MR imaging, adenomas demonstrate variable signal intensity depending on lipid content and presence of hemorrhage. At T1WI, adenomas can be isointense to hyperintense due to lipid content or hemorrhage. High signals from lipid content drop out at T1WI OP imaging (Figure 4), while high signals from hemorrhage persist. They have variable signal intensity at T2WI and DWI. At

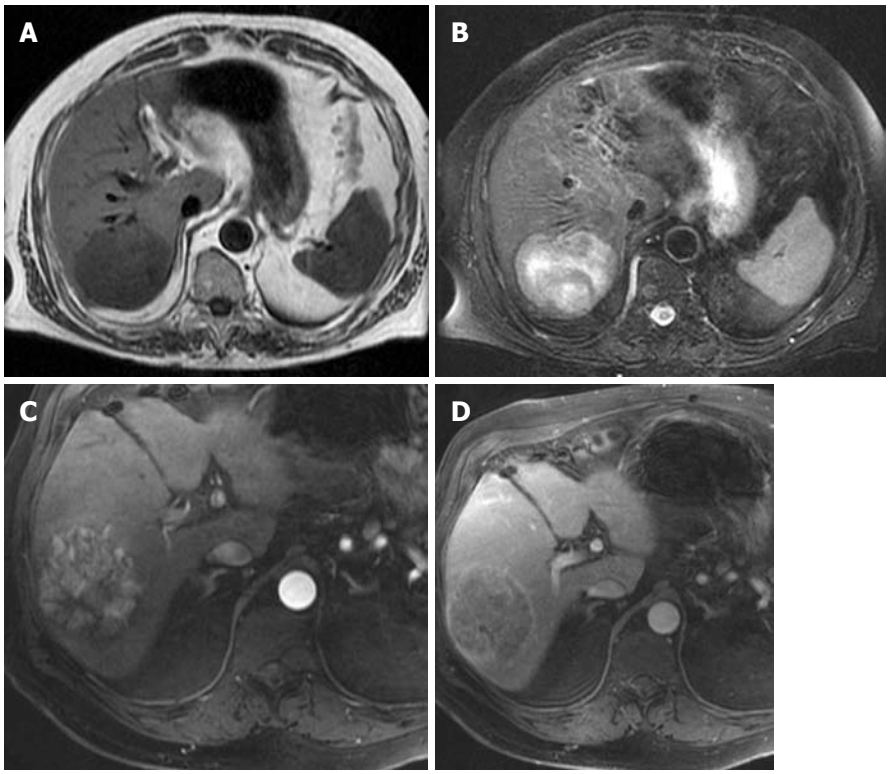

Figure 5 A 65-year-old male with hepatocellular carcinoma. A: T1 weighted imaging in phase image shows a hypointense mass in the right lobe of the liver; B: T2 weighted imaging (TE = 85 ms) shows a hyperintense mass in the right lobe of the liver; C, D: Late arterial (C) and excretory phase (D) shows a hypervascular mass in the liver that demonstrates an enhancing capsule on the delayed images.

DCE-MRI, they can have heterogeneous early enhancement during the arterial phase with variable degrees of washout on the venous and delayed phases (Figure 4). A peripheral delayed enhancement of the pseudocapsule can be seen. At the hepatocyte phase, even though an adenoma takes up minimal to moderate amounts of contrast relative to the surrounding liver, the adenoma will commonly appear hypointense due to the absence of biliary ducts resulting in no contrast being excreted or accumulated prior to drainage[19].

Hepatocellular carcinoma

Hepatocellular carcinoma (HCC) is the most common primary liver malignancy. HCC most commonly develops in the background of chronic liver disease, ending in cirrhosis due to various etiologies including viral hepatitis, alcohol, hematochromatosis and Wilson's disease. HCC typically develops in a stepwise manner that begins with regenerative nodules (RN) (non-premalignant), to dysplastic nodules (DN, pre-malignant), to DN with HCC, to HCC. HCCs can be solitary (50%), multifocal (40%) or diffuse (less than 10%)[30]. MRI plays an important role in differentiating these non malignant nodules from HCC[31-33]. At MR imaging, HCCs have variable appearances but usually they are hypointense on T1WI and mild to moderately hyperintense on T2WI. Smaller HCCs (< 2.0 cm) are frequently isointense on both T1WI and T2WI[30,34]. At DCE-MRI, HCCs demonstrate classic intense early arterial enhancement that washes out in the equilibrium phase (Figure 5). The majority of HCCs have a capsule consisting of compressed liver parenchyma that usually enhances on the delayed images. Some DN can mimic HCCs with intense early arterial enhancement, however, they do not show the typical washout in the equilibrium phase or increased signal on T2WI. The hepatocyte phase has been evaluated in the setting of HCC. Most hepatomas are hypointense to liver in this phase of contrast administration. This is a function of organic anion transport function rather than stage of tumor differentiation[30,34,35].

Intrahepatic cholangiocarcinoma

Intrahepatic cholangiocarcinoma (IHCC) is the second most common primary liver malignancy, after HCC. IHCCs are part of a spectrum of cholangiocarcinoma tumors of the biliary epithelium. Cholangiocarcinoma tumors are classified based on the site of origin: intrahepatic, gallbladder, or extrahepatic biliary cancers. At MR imaging, IHCC is iso- to hypointense on T1WI and mild to marked hyperintense on T2WI (Figure 6). Appearance on T2WI and DWI can vary depending on its content: amount of fibrous content (predominant central hypointensity) and mucin content (hyperintense). On the DWI, IHCC that exhibits restrictive diffusion will have no signal drop on high b-value imaging. At DCE-MRI, IHCC demonstrates incomplete arterial enhancement (Figure 6). On delayed images, mild progressive enhancement is usually observed[3,30,36]. During the hepatocyte phase of contrast administration, IHCCs are hypointense to liver (Figure 7).

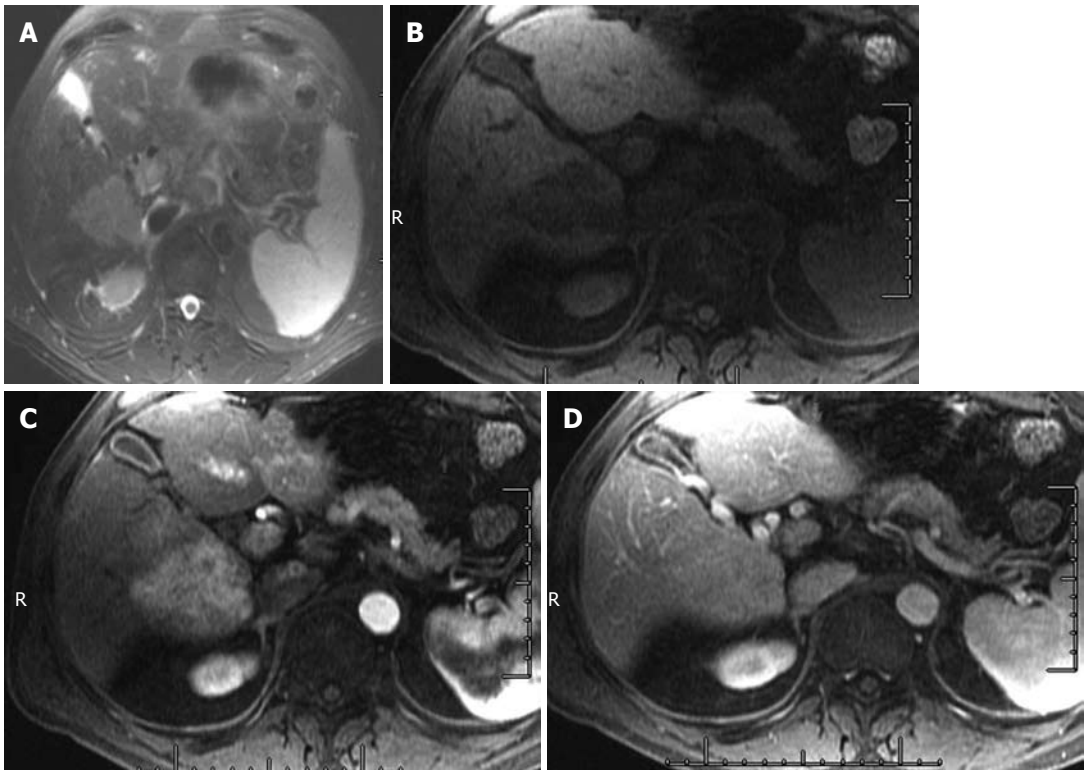

Figure 6 A 62-year-old male with intrahepatic cholangiocarcinoma. A: Short TE (85 ms) T2 weighted imaging shows a hyperintense mass in the right lobe of the liver; B-D: Pre-contrast (B) late arterial (C), and 5 min delayed images (D) of the abdomen shows delayed enhancement.

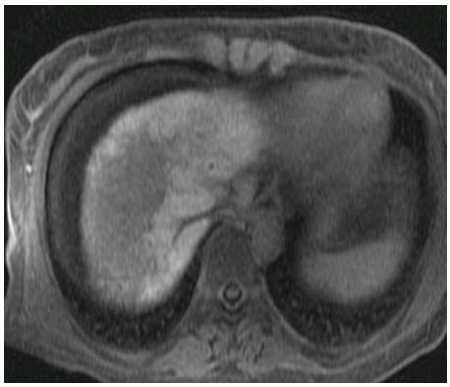

Figure 7 A 54-year-old female with intrahepatic cholangiocarcinoma. The hepatocyte phase of contrast administration shows no uptake of contrast.

Liver metastases

Metastases are the most common malignant liver lesions, with colorectal cancer as the most common primary malignancy. All metastatic liver lesions, with the exception of highly cystic or necrotic lesions, have variable degrees of vascularity and can be classified into hypovascular and hypervascular metastases. This refers to the vascularity of the lesions relative to the vascularity of surrounding liver parenchyma[24,27].

Hypervascular liver metastases

Metastases that are considered hypervascular typically arise from thyroid carcinoma, carcinoid tumor, neuroendocrine tumor, renal cell carcinoma, choriocarcinoma, melanoma and sarcomas. At MR imaging, these metastases generally have variable appearances on both T1WI and T2WI. On T1WI, metastases are usually mildly to moderately hypointense relative to liver parenchyma. Some intralesional substances such as hemorrhage, melanin, fat and protein can cause shortening of T1 relaxation times resulting in hyperintense metastatic lesions on T1WI. On T2WI, liver metastases are hyperintense relative to liver but generally less hyperintense than cysts and hemangioma. The difference in CNR between the metastases and these benign lesions can be highlighted on longer TE where signal attenuation is observed with metastases and hyperintensity accentuation is observed with cysts and hemangioma. However, a subset of metastases that include neuroendocrine tumors, sarcomas and melanoma can appear cystic and markedly hyperintense on T2WI without signal attenuation at longer TE, thus mimicking simple cysts and hemangioma[27,37]. At DWI, these cystic metastases are usually hyperintense on low b-values with variable degrees of signal attenuation at high b-values. On the contrary, solid metastatic lesions will remain hyperintense at high b-values due to restrictive diffusion (Figure 8)[38,39]. Dynamic enhancement patterns also play a critical role in distinguishing these lesions.

Variable early arterial enhancement at the DCE-MRI has been observed that includes peripheral ring and homogenous and heterogeneous enhancement. The peripheral ring pattern is the most commonly described enhancement pattern. Homogenous arterial enhancement is usually seen in smaller hypervascular metastases (< 1.5 cm). Heterogeneous enhancement can be seen in lesions larger than

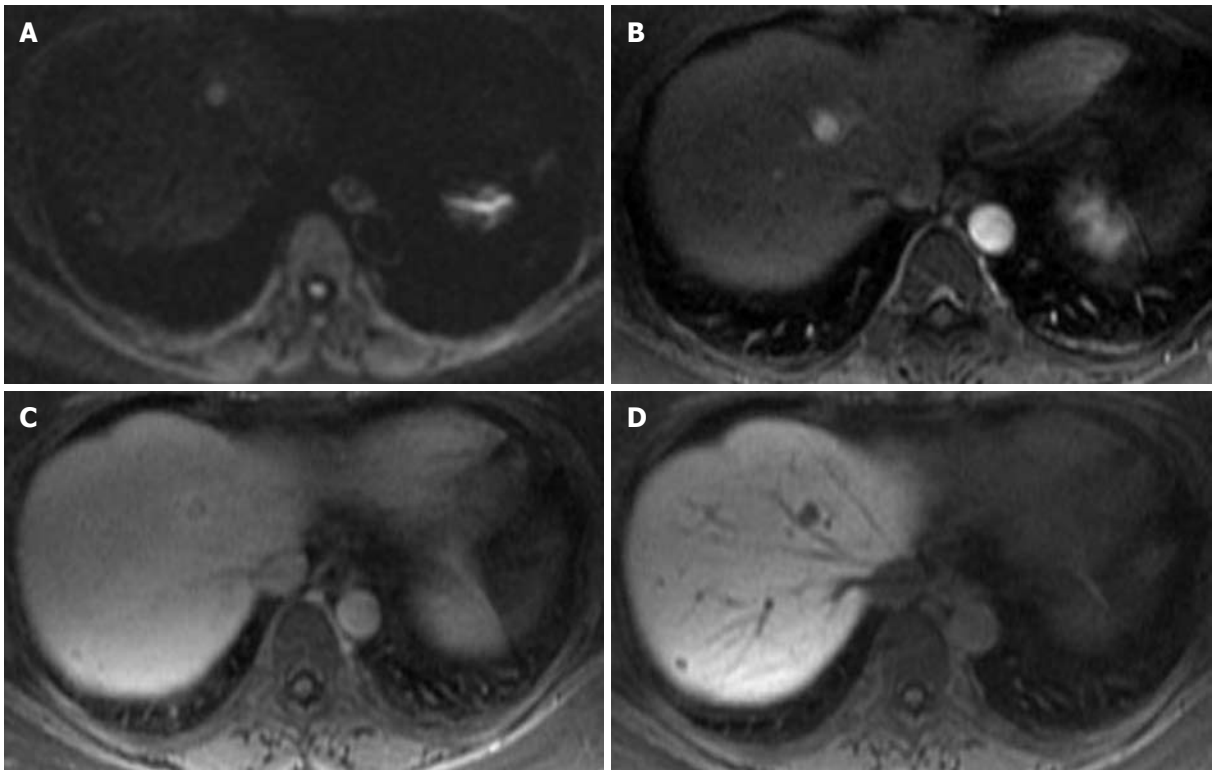

Figure 8 A 51-year-old female with metastatic liver lesions from a pancreatic primary. A: The diffusion weighted imaging at b = 500 shows two hyperintense nodules in the liver, in keeping with solid lesions; B, C: The late arterial phase (B) shows hypervascular masses that washout on the excretory phase (C) of contrast administration; D: The hepatocyte phase shows low signal lesions in the right lobe of the liver, corresponding to liver metastases.

3 cm that are complicated by intralesional hemorrhage, necrosis and fibrotic tissue formation. On the delayed images, most hypervascular metastases demonstrate incomplete enhancement due to poor central vascularity with simultaneous peripheral washout. The peripheral washout observed on the delayed images is considered specific for liver malignancies that include metastases and HCC (Figure 8). Hepatocyte contrast agent provides increased conspicuity on the 20 min hepatocyte phase images, while liver metastases do not take up contrast (Figure 8)[30]. In some series, there are reports of increased lesion detection that affected decision making and the clinical approach to the patient.

Hypovascular liver metastases

Metastases that are considered hypovascular are most commonly from colon carcinoma. Other less common primary lesions include: bladder carcinoma, prostate carcinoma, and pulmonary carcinoma[40]. At MR imaging, hypovascular metastases have variable appearances on both T1WI and T2WI, which are commonly mild to moderately hypointense on T1WI and hyperintense on T2WI, with variability in signal intensity due to the presence of intralesional substances. At DCE MRI, hypovascular metastases generally demonstrate variable enhancement in the arterial phase with the most common pattern being peripheral complete ring enhancement (Figure 9). Hypovascular metastases generally demonstrate a lesser degree of enhancement relative to the surrounding liver parenchyma. Occasionally, transient perilesional circumferential or wedge-shaped enhancements are seen in the arterial phase, most commonly with colorectal metastases[3,27,40]. Hypovascular metastases are conspicuous on the portal venous phase as hypointense lesions relative to the liver[27]. On the excretory phase, peripheral washout is commonly observed (Figure 9)[40]. The hepatocyte agents provide high CNR and sensitivity for liver metastasis at 20 min[30]. In this phase, these masses will appear hypointense to liver.

Arterially enhancing nodules

Liver lesions are typically classified as hypervascular and hypovascular based on their enhancement pattern on the arterial phase of DCE-MRI. The arterial phase is highly sensitive in detecting hypervascular lesions but may have a low specificity in lesion characterization. The arterial enhancing nodule (AEN) can be true masses with mass effect and rounded/lobulated shapes. These are seen only during the arterial phase of contrast administration. AEN can also be pseudolesions that mimic masses without a mass effect. To confidently distinguish between benign and malignant processes and possibly arrive at a correct diagnosis, the AEN enhancement characteristics should be evaluated in conjunction with other MRI imaging features[41].

Differential diagnoses of benign AEN include hepatocellular adenoma, FNH, hemangiomas, transient hepatic intensity differences, and arteriovenous shunts/perfusion anomalies. The differential diagnosis includes malignant processes such as HCC and hypervascular me-

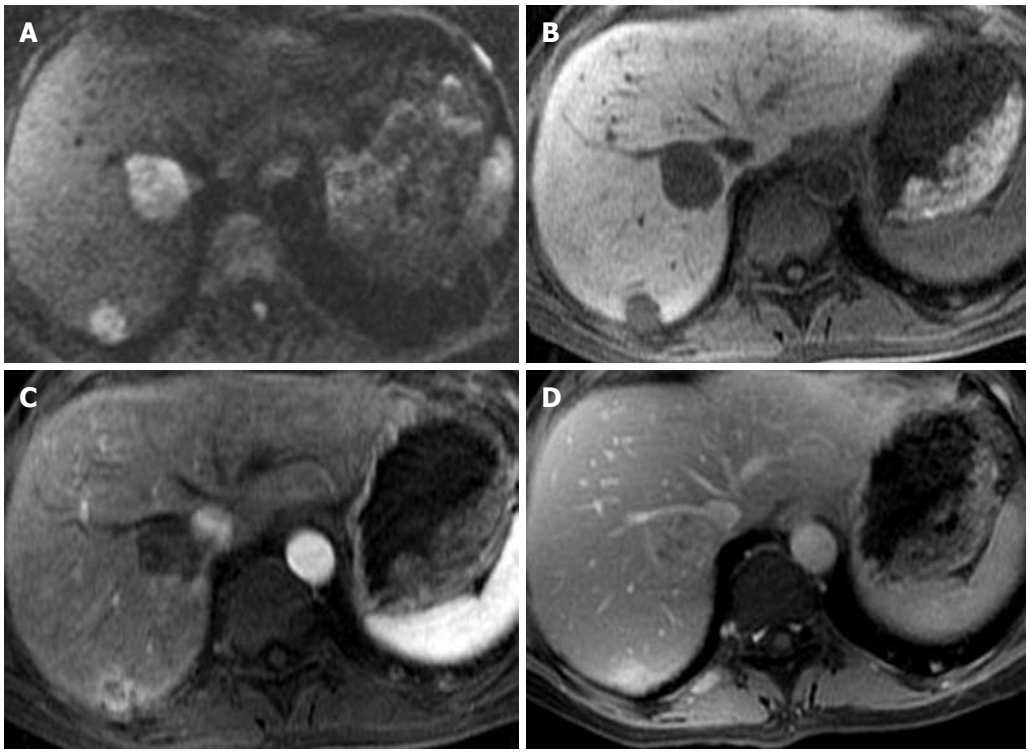

Figure 9 A 64-year-old with liver metastases from a primary sarcoma. A: The diffusion weighted imaging at b = 500 shows two solid lesions in the right lobe of the liver; B-D: The pre-contrast (B), late arterial (C), and delayed phase (D) show late enhancement. The enhancement pattern is similar to intrahepatic cholangiocarcinoma.

tastasis[42]. Even in the setting of a cirrhotic liver, these lesions are more likely to be benign in nature[10,41-43]. Imaging features that suggest a malignant process include hyperintense signal on the T2WI and washout on the delayed phase of contrast administration. A smaller lesion (< 5 mm) should be monitored at least at 6 mo intervals, whereas a larger lesion (> 1 cm) should be monitored every 3 mo for interval size change or signal changes on the T2WI.

DIFFUSE LIVER DISEASE

Fatty liver disease

In the United States, fatty liver disease (FLD) is the leading cause of chronic liver disease in the adult and pediatric populations[44]. Two conditions commonly associated with FLD are alcoholic abuse and non alcoholic FLD (NAFLD)[45]. NAFLD is expected to surpass chronic hepatitis C as the number one indication for liver transplantation[25]. NAFLD is closely linked to metabolic syndromes that encompass constellations of metabolic abnormalities that include type II diabetes mellitus, obesity, hyperlipidemia, and insulin resistance[6,25]. Other conditions that can result in NAFLD include drug toxicity (such as amiodarone, tamoxifen and antiretrovirals), viral hepatitis, radiation therapy, and storage disease such as glycogen storage disorder. Patterns of fatty deposition in FLD is commonly diffuse deposition, and less commonly focal fat deposition in normal liver and diffuse fat deposition with focal sparing. NAFLD comprises a spectrum of liver pathologies that range from simple steatosis to nonalcoholic steatohepatitis that may further progress to fibrosis and cirrhosis with resultant increased risk for HCC development and liver failure[25,46]. Histopathologic hallmarks of simple steatosis that represents 80%-90% of NAFLD cases is fat accumulation within the liver cells. The current standard of reference for detection and disease severity of FLD assessment is liver biopsy, which is invasive, costly and is associated with complications and high sampling error due to heterogeneous fat distribution that can be seen with FLD. Noninvasive repeat evaluation of fatty liver for monitoring of treatment response is often desired.

At MR imaging, areas of fat deposition in the liver appear isointense or hyperintense to the liver on the IP T1WI. On the opposed-phase T1WI, these areas demonstrate signal loss (Figure 10). Diffuse liver steatosis will demonstrate diffuse heterogeneous, or more commonly homogenous signal loss, on the opposed phase. Wedged shaped, geographic or nodular morphology of focal FLD allows for distinction from fat containing tumors, such as HCC, adenoma, angiomyolipoma or lipoma. At DCE MRI, focal FLD will not demonstrate a mass effect on adjacent vessels or biliary tract, or changes in CNR relative to liver[47]. Patchy enhancement of the liver parenchyma, sometimes seen on the arterial phase, that becomes isointense to surrounding liver parenchyma at delayed imaging are considered indicators of areas with necro-inflammatory activity[48]. It is important to note that accumulation of iron (patients with hemochromatosis) or glycogen (patients with glycogen storage disease) in the liver cells can alter signal intensity or signal loss of fatty liver in patients with concomitant FLD[44].

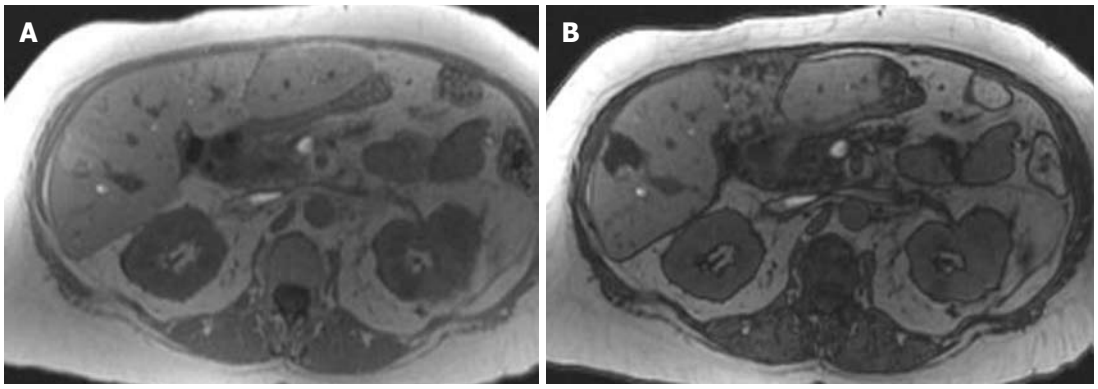

Figure 10 A 57-year-old female with breast cancer with focal fat deposition in the liver. The in-phase (A) and out-of-phase (B) images show a signal drop of the area in segment Ⅴ of the liver.

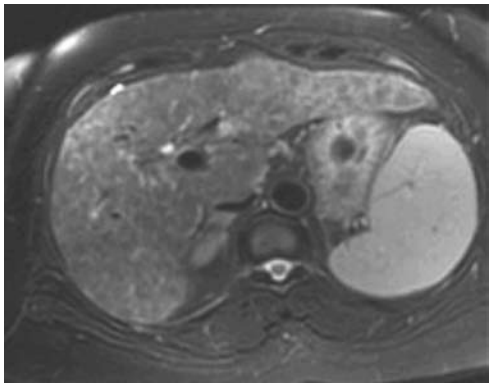

Figure 11 A 57-year-old female with hepatocellular carcinoma and liver cirrhosis. The T2 weighted imaging shows enlargement of the lateral segment of the left lobe of the liver and caudate lobe. There is a nodular contour of the liver. All these findings are in keeping with cirrhosis. The spleen is enlarged in keeping with portal hypertension.

Cirrhosis

Hepatic fibrosis is a dynamic process that is usually induced by a nonspecific inflammatory response of hepatocytes to hepatocellular injury (hepatitis) due to numerous etiologies such as hepatitis viruses (B and C), alcohol abuse, autoimmune disease, drug toxicity, radiation therapy and metabolic disorders such as NAFLD and hemochromatosis[19,49-52]. Cirrhosis progresses from chronic hepatitis to early cirrhosis to advanced cirrhosis, which are initially compensated, and later progresses to decompensated cirrhosis to finally end-stage cirrhosis.

The morphological changes seen on imaging in a patient with cirrhosis include a nodular liver and enlargement of the left lobe and caudate lobe (Figure 11). A right hepatic notch and enlarged gallbladder fossa have been described in patients with cirrhosis[19,49-52].

Extrahepatic findings associated with decompensated cirrhosis are mainly features associated with portal hypertension that include splenomegaly (Figure 11), ascites, portosystemic collateral vessels and nonspecific periportal and portocaval lymphadenopathy (greater than 1 cm in the short axis). Findings related to hepatocellular dysfunction with resultant metabolic abnormality, causing small bowel edema and gallbladder wall thickening, are also observed. Spleen size greater than 13 cm in cephalocaudal indicates splenomegaly. The presences of 3-8 mm hemosiderin containing nodules called Gamna-Gandy are indirect signs of portal hypertension. These nodules result from hypertensive bleeding in the splenic follicles[10,48].

The current standard of reference for the diagnosis of cirrhosis is liver biopsy, which has its inherent limitations due to sampling error and post procedural complications. MRI has emerged as a relatively safer, inexpensive and comprehensive alternative method for the detection and evaluation of cirrhosis[53]. At MRI, liver fibrosis demonstrates imaging patterns that range from an absent distinct pattern, reticular, confluent or both reticular and confluent patterns[48]. The fibrous septa and bridges in cirrhosis appear as hypointense on T1WI and hyperintense on T2W1. These signal characteristics are due to inflammatory changes, vascular dilation and and/or development of pseudobile ducts. The RN typically appear intermediate to hyperintense on T1WI and intermediate to hypointense on T2WI. Some of these RNs accumulate iron (called siderotic nodules) and will appear strikingly hypointense on T2- and T2WI. There also RNs that accumulate fat (called steatotic nodules) and tend to show signal loss on the OP images. It is worth noting that the fibrous septa and bridges lack iron or fat in either the patients with iron or fat deposition because both diseases are an intracellular deposition phenomenon[38,40,49]. At DCE-MRI with nonspecific GBCA, liver fibrosis demonstrates no significant enhancement in the arterial and early venous phases. Delayed progressive enhancement with peaks in the late venous and equilibrium phases is typically observed. This delayed enhancement pattern can be explained by the characteristic accumulation of nonspecific GDBA in the extracellular spaces that are abundant in the fibrous tissues. In contrast to reticular fibrosis that is linear reticulations surrounding RNs, confluent fibrosis is thicker fibrotic scars up to several centimeters thick with masslike configurations. Confluent fibrosis has signal intensity and an enhancement pattern similar to reticular type liver fibrosis. Occasionally, arterial enhancement is seen with confluent and reticular type fibrosis that can be differentiated from other

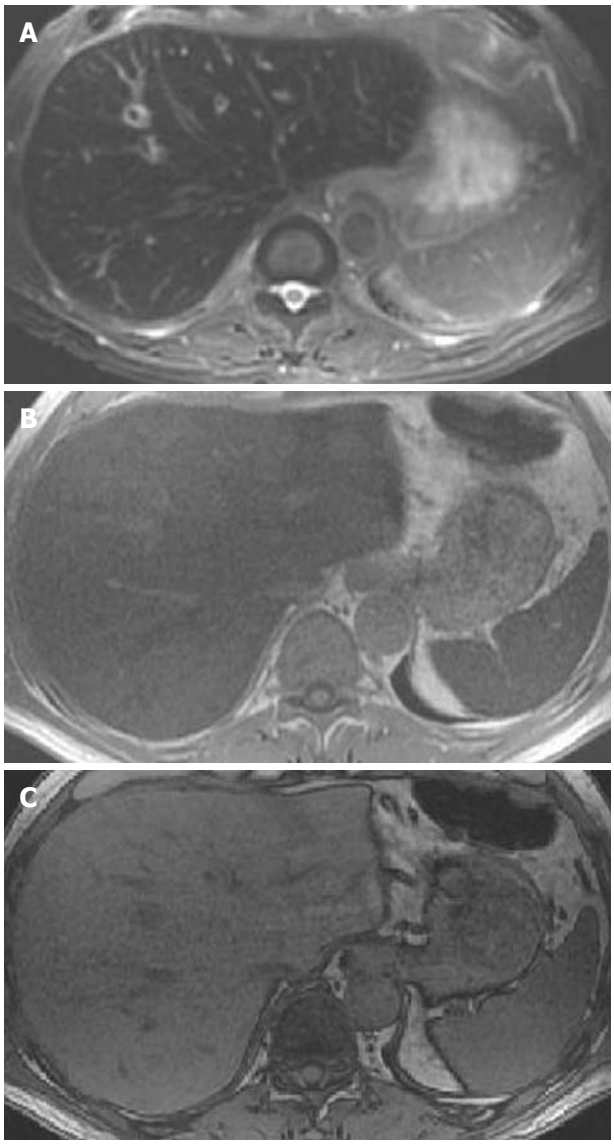

Figure 12 A 64-year-old male with a pancreatic mass and iron deposition in the liver. A: Respiratory triggered fast spin echo T2 weighted imaging image of the liver shows a darker liver relative to the muscles; B, C: In phase (B) and out-of-phase (C) T1 weighted imaging shows a signal drop on the former in keeping with iron deposition.

focal liver tumors based on the characteristic morphology and persistent enhancement on subsequent phases. At the hepatocyte phase, liver fibrosis has no contrast uptake and therefore will appear hypointense[48,49].

Hemochromatosis

Hemochromatosis can be categorized into primary or secondary disorders based on the causes. This disease results in increased intestinal iron absorption with normal dietary iron intake. The excess iron in primary hemochromatosis is deposited in parenchymal cells in organs such as liver, pancreas, heart, pituitary gland, thyroid and synovium[54]. Non genetic causes classified as secondary hemochromatosis include ineffective erythropoiesis disorders such as thalassemia, myelodysplastic syndrome, anemia due to chronic disease, cirrhosis related iron deposition and exogenous increase by multiple transfusions. In the liver, excessive iron deposition results in cellular damage that can lead to cirrhosis and its complication, such as portal hypertension and the development of HCC. In secondary hemochromatosis, excess iron is deposited in the reticuloendothelial system, such as spleen, bone marrow, and liver with minimal cellular damage. Hence, hemochromatosis can also be categorized into parenchymal and reticuloendothelial forms based of the distribution of the iron deposition. In general, hemochromatosis is a clinically silent disease. The laboratory values used to diagnosis this disease have low sensitivity and specificity. Liver biopsy is the standard of reference for diagnosis that comes with its inherent sampling error and complications. MRI is a good noninvasive alternative method for the detection, diagnosis and monitoring of treatment response[54].

Utilizing a core MR-protocol with the axial T1 weighted SPGR IP and OP imaging, liver parenchyma with excess intracellular iron deposition shows signal loss on the IP images with longer echo times. This signal loss due to susceptibility effects of iron are more pronounced at longer echo times (Figure 12). A caveat of this technique is that, in patients with both diffuse steatosis and hemochromatosis diseases, theoretically no signal loss will be detected on the IP and OP images[55]. The distribution of iron deposition based on signal loss observed on the IP images can help distinguish primary and secondary hemochromatosis. In primary hemochromatosis, both the liver and pancreas will show signal loss, while signal intensity in the spleen and bone marrow will be unchanged. In secondary hemochromatosis, signal loss will be seen in the liver, spleen and bone marrow, while the signal intensity of the pancreas will preserved[54]. If there is a clinical suspicion of hemochromatosis, multiple TEs can be obtained on GRE sequences and the degree of iron overload can be calculated from the rate of signal loss as a function of TE[56].

CONCLUSION

Liver MRI is rapidly becoming the first image modality of choice for the clinician in the evaluation of liver masses and diffused liver disease. We have presented a core imaging protocol with a combination of T1, including in-and out-of phase imaging, T2, DWI EPI and dynamic post-Gd images with and without hepatocyte agents to evaluate the liver. Utilizing this basic protocol, most of the benign and malignant liver lesions can be characterized and, in addition, underlying liver disease can be identified. In the coming months, new innovative techniques will used more expansively, such as elastography, and will improve the role of MRI in liver imaging.

REFERENCES

1 **Martin DR**, Semelka RC. Magnetic resonance imaging of the liver: review of techniques and approach to common diseases. *Semin Ultrasound CT MR* 2005; **26**: 116-131

2 **Honal M**, Bauer S, Ludwig U, Leupold J. Increasing efficiency of parallel imaging for 2D multislice acquisitions. *Magn*

Reson Med 2009; **61**: 1459-1470
3 **Low RN**. Abdominal MRI advances in the detection of liver tumours and characterisation. *Lancet Oncol* 2007; **8**: 525-535
4 **Zech CJ**, Grazioli L, Breuer J, Reiser MF, Schoenberg SO. Diagnostic performance and description of morphological features of focal nodular hyperplasia in Gd-EOB-DTPA-enhanced liver magnetic resonance imaging: results of a multicenter trial. *Invest Radiol* 2008; **43**: 504-511
5 **Larkman DJ**, Nunes RG. Parallel magnetic resonance imaging. *Phys Med Biol* 2007; **52**: R15-R55
6 **Hines CD**, Yu H, Shimakawa A, McKenzie CA, Warner TF, Brittain JH, Reeder SB. Quantification of hepatic steatosis with 3-T MR imaging: validation in ob/ob mice. *Radiology* 2010; **254**: 119-128
7 **Li T**, Mirowitz SA. Fast T2-weighted MR imaging: impact of variation in pulse sequence parameters on image quality and artifacts. *Magn Reson Imaging* 2003; **21**: 745-753
8 **Bayramoglu S**, Kilickesmez O, Cimilli T, Kayhan A, Yirik G, Islim F, Alibek S. T2-weighted MRI of the upper abdomen: comparison of four fat-suppressed T2-weighted sequences including PROPELLER (BLADE) technique. *Acad Radiol* 2010; **17**: 368-374
9 **Akin O**, Schwartz LH, Welber A, Maier CF, Decorato DR, Panicek DM. Evaluation of focal liver lesions: fast-recovery fast spin echo T2-weighted MR imaging. *Clin Imaging* 2006; **30**: 322-325
10 **Mortelé KJ**, Ros PR. Cystic focal liver lesions in the adult: differential CT and MR imaging features. *Radiographics* 2001; **21**: 895-910
11 **Koh DM**, Collins DJ. Diffusion-weighted MRI in the body: applications and challenges in oncology. *AJR Am J Roentgenol* 2007; **188**: 1622-1635
12 **Koike N**, Cho A, Nasu K, Seto K, Nagaya S, Ohshima Y, Ohkohchi N. Role of diffusion-weighted magnetic resonance imaging in the differential diagnosis of focal hepatic lesions. *World J Gastroenterol* 2009; **15**: 5805-5812
13 **Sandrasegaran K**, Akisik FM, Lin C, Tahir B, Rajan J, Aisen AM. The value of diffusion-weighted imaging in characterizing focal liver masses. *Acad Radiol* 2009; **16**: 1208-1214
14 **Blaimer M**, Breuer F, Mueller M, Heidemann RM, Griswold MA, Jakob PM. SMASH, SENSE, PILS, GRAPPA: how to choose the optimal method. *Top Magn Reson Imaging* 2004; **15**: 223-236
15 **Brau AC**, Beatty PJ, Skare S, Bammer R. Comparison of reconstruction accuracy and efficiency among autocalibrating data-driven parallel imaging methods. *Magn Reson Med* 2008; **59**: 382-395
16 **Margolis DJ**, Bammer R, Chow LC. Parallel imaging of the abdomen. *Top Magn Reson Imaging* 2004; **15**: 197-206
17 **Yoshioka H**, Takahashi N, Yamaguchi M, Lou D, Saida Y, Itai Y. Double arterial phase dynamic MRI with sensitivity encoding (SENSE) for hypervascular hepatocellular carcinomas. *J Magn Reson Imaging* 2002; **16**: 259-266
18 **Kanematsu M**, Goshima S, Kondo H, Yokoyama R, Kajita K, Hoshi H, Onozuka M, Nozaki A, Hirano M, Shiratori Y, Moriyama N. Double hepatic arterial phase MRI of the liver with switching of reversed centric and centric K-space reordering. *AJR Am J Roentgenol* 2006; **187**: 464-472
19 **Sharma P**, Kitajima HD, Kalb B, Martin DR. Gadolinium-enhanced imaging of liver tumors and manifestations of hepatitis: pharmacodynamic and technical considerations. *Top Magn Reson Imaging* 2009; **20**: 71-78
20 **Motosugi U**, Ichikawa T, Tominaga L, Sou H, Sano K, Ichikawa S, Araki T. Delay before the hepatocyte phase of Gd-EOB-DTPA-enhanced MR imaging: is it possible to shorten the examination time? *Eur Radiol* 2009; **19**: 2623-2629
21 **Reimer P**, Schneider G, Schima W. Hepatobiliary contrast agents for contrast-enhanced MRI of the liver: properties, clinical development and applications. *Eur Radiol* 2004; **14**: 559-578
22 **Seale MK**, Catalano OA, Saini S, Hahn PF, Sahani DV. Hepatobiliary-specific MR contrast agents: role in imaging the liver and biliary tree. *Radiographics* 2009; **29**: 1725-1748
23 **Tanimoto A**, Lee JM, Murakami T, Huppertz A, Kudo M, Grazioli L. Consensus report of the 2nd International Forum for Liver MRI. *Eur Radiol* 2009; **19** Suppl 5: S975-S989
24 **Tamada T**, Ito K, Sone T, Yamamoto A, Yoshida K, Kakuba K, Tanimoto D, Higashi H, Yamashita T. Dynamic contrast-enhanced magnetic resonance imaging of abdominal solid organ and major vessel: comparison of enhancement effect between Gd-EOB-DTPA and Gd-DTPA. *J Magn Reson Imaging* 2009; **29**: 636-640
25 **Taouli B**, Ehman RL, Reeder SB. Advanced MRI methods for assessment of chronic liver disease. *AJR Am J Roentgenol* 2009; **193**: 14-27
26 **Taouli B**, Vilgrain V, Dumont E, Daire JL, Fan B, Menu Y. Evaluation of liver diffusion isotropy and characterization of focal hepatic lesions with two single-shot echo-planar MR imaging sequences: prospective study in 66 patients. *Radiology* 2003; **226**: 71-78
27 **Silva AC**, Evans JM, McCullough AE, Jatoi MA, Vargas HE, Hara AK. MR imaging of hypervascular liver masses: a review of current techniques. *Radiographics* 2009; **29**: 385-402
28 **Kamaya A**, Maturen KE, Tye GA, Liu YI, Parti NN, Desser TS. Hypervascular liver lesions. *Semin Ultrasound CT MR* 2009; **30**: 387-407
29 **Hardie AD**, Naik M, Hecht EM, Chandarana H, Mannelli L, Babb JS, Taouli B. Diagnosis of liver metastases: value of diffusion-weighted MRI compared with gadolinium-enhanced MRI. *Eur Radiol* 2010; **20**: 1431-1441
30 **Ba-Ssalamah A**, Uffmann M, Saini S, Bastati N, Herold C, Schima W. Clinical value of MRI liver-specific contrast agents: a tailored examination for a confident non-invasive diagnosis of focal liver lesions. *Eur Radiol* 2009; **19**: 342-357
31 **Forner A**, Vilana R, Ayuso C, Bianchi L, Solé M, Ayuso JR, Boix L, Sala M, Varela M, Llovet JM, Brú C, Bruix J. Diagnosis of hepatic nodules 20 mm or smaller in cirrhosis: Prospective validation of the noninvasive diagnostic criteria for hepatocellular carcinoma. *Hepatology* 2008; **47**: 97-104
32 **Krinsky G**. Imaging of dysplastic nodules and small hepatocellular carcinomas: experience with explanted livers. *Intervirology* 2004; **47**: 191-198
33 **Roncalli M**, Borzio M, Di Tommaso L. Hepatocellular dysplastic nodules. *Hepatol Res* 2007; **37** Suppl 2: S125-S134
34 **Choi BI**, Lee JM. Advancement in HCC imaging: diagnosis, staging and treatment efficacy assessments : Imaging diagnosis and staging of hepatocellular carcinoma. *J Hepatobiliary Pancreat Sci* 2010; **17**: 369-373
35 **Frericks BB**, Loddenkemper C, Huppertz A, Valdeig S, Stroux A, Seja M, Wolf KJ, Albrecht T. Qualitative and quantitative evaluation of hepatocellular carcinoma and cirrhotic liver enhancement using Gd-EOB-DTPA. *AJR Am J Roentgenol* 2009; **193**: 1053-1060
36 **Jang HJ**, Yu H, Kim TK. Imaging of focal liver lesions. *Semin Roentgenol* 2009; **44**: 266-282
37 **Kelekis NL**, Semelka RC, Woosley JT. Malignant lesions of the liver with high signal intensity on T1-weighted MR images. *J Magn Reson Imaging* 1996; **6**: 291-294
38 **Parikh T**, Drew SJ, Lee VS, Wong S, Hecht EM, Babb JS, Taouli B. Focal liver lesion detection and characterization with diffusion-weighted MR imaging: comparison with standard breath-hold T2-weighted imaging. *Radiology* 2008; **246**: 812-822
39 **Taouli B**, Koh DM. Diffusion-weighted MR imaging of the liver. *Radiology* 2010; **254**: 47-66
40 **Danet IM**, Semelka RC, Leonardou P, Braga L, Vaidean G, Woosley JT, Kanematsu M. Spectrum of MRI appearances of untreated metastases of the liver. *AJR Am J Roentgenol* 2003; **181**: 809-817
41 **Brancatelli G**, Federle MP, Baron RL, Lagalla R, Midiri M,

Vilgrain V. Arterially enhancing liver lesions: significance of sustained enhancement on hepatic venous and delayed phase with magnetic resonance imaging. *J Comput Assist Tomogr* 2007; **31**: 116-124
42 **Iannaccone R**, Federle MP, Brancatelli G, Matsui O, Fishman EK, Narra VR, Grazioli L, McCarthy SM, Piacentini F, Maruzzelli L, Passariello R, Vilgrain V. Peliosis hepatis: spectrum of imaging findings. *AJR Am J Roentgenol* 2006; **187**: W43-W52
43 **Mortele KJ**, Ros PR. MR imaging in chronic hepatitis and cirrhosis. *Semin Ultrasound CT MR* 2002; **23**: 79-100
44 **Zhong L**, Chen JJ, Chen J, Li L, Lin ZQ, Wang WJ, Xu JR. Nonalcoholic fatty liver disease: quantitative assessment of liver fat content by computed tomography, magnetic resonance imaging and proton magnetic resonance spectroscopy. *J Dig Dis* 2009; **10**: 315-320
45 **Schwenzer NF**, Machann J, Martirosian P, Stefan N, Schraml C, Fritsche A, Claussen CD, Schick F. Quantification of pancreatic lipomatosis and liver steatosis by MRI: comparison of in/opposed-phase and spectral-spatial excitation techniques. *Invest Radiol* 2008; **43**: 330-337
46 **Reeder SB**, Robson PM, Yu H, Shimakawa A, Hines CD, McKenzie CA, Brittain JH. Quantification of hepatic steatosis with MRI: the effects of accurate fat spectral modeling. *J Magn Reson Imaging* 2009; **29**: 1332-1339
47 **Basaran C**, Karcaaltincaba M, Akata D, Karabulut N, Akinci D, Ozmen M, Akhan O. Fat-containing lesions of the liver: cross-sectional imaging findings with emphasis on MRI. *AJR Am J Roentgenol* 2005; **184**: 1103-1110
48 **Elias J Jr**, Altun E, Zacks S, Armao DM, Woosley JT, Semelka RC. MRI findings in nonalcoholic steatohepatitis: correlation with histopathology and clinical staging. *Magn Reson Imaging* 2009; **27**: 976-987
49 **Faria SC**, Ganesan K, Mwangi I, Shiehmorteza M, Viamonte B, Mazhar S, Peterson M, Kono Y, Santillan C, Casola G, Sirlin CB. MR imaging of liver fibrosis: current state of the art. *Radiographics* 2009; **29**: 1615-1635
50 **Ito K**, Mitchell DG. Hepatic morphologic changes in cirrhosis: MR imaging findings. *Abdom Imaging* 2000; **25**: 456-461
51 **Ito K**, Mitchell DG. Imaging diagnosis of cirrhosis and chronic hepatitis. *Intervirology* 2004; **47**: 134-143
52 **Ito K**, Mitchell DG, Siegelman ES. Cirrhosis: MR imaging features. *Magn Reson Imaging Clin N Am* 2002; **10**: 75-92, vi
53 **Mortelé KJ**, Praet M, Van Vlierberghe H, de Hemptinne B, Zou K, Ros PR. Focal nodular hyperplasia of the liver: detection and characterization with plain and dynamic-enhanced MRI. *Abdom Imaging* 2002; **27**: 700-707
54 **Queiroz-Andrade M**, Blasbalg R, Ortega CD, Rodstein MA, Baroni RH, Rocha MS, Cerri GG. MR imaging findings of iron overload. *Radiographics* 2009; **29**: 1575-1589
55 **Merkle EM**, Nelson RC. Dual gradient-echo in-phase and opposed-phase hepatic MR imaging: a useful tool for evaluating more than fatty infiltration or fatty sparing. *Radiographics* 2006; **26**: 1409-1418
56 **Alexopoulou E**, Stripeli F, Baras P, Seimenis I, Kattamis A, Ladis V, Efstathopoulos E, Brountzos EN, Kelekis AD, Kelekis NL. R2 relaxometry with MRI for the quantification of tissue iron overload in beta-thalassemic patients. *J Magn Reson Imaging* 2006; **23**: 163-170

S- Editor Cheng JX **L- Editor** Lutze M **E- Editor** Zheng XM